Speed Control of a Three-Phase Induction Motor Based on Robust Optimal Preview Control Theory

Mohamed M. M. Negm, *Senior Member, IEEE*, Jamil M. Bakhashwain, and M. H. Shwehdi, *Senior Member, IEEE*

***Abstract*—A synthesized method for speed control of a three-phase induction motor (IM) based on optimal preview control system theory is implemented in this article. An IM model comprises three-input variables and three-output variables that coincide with the synchronous reference frame that is implemented using the vector method. The input variables of this model are the stator angular frequency and the two components of the stator space voltage vector, whereas the output variables are the rotor angular speed and the two components of the stator space flux linkage. The objective of the synthesized control system is to achieve motor speed control, field orientation control, and constant flux control. A novel error system is derived and introduced into the control law to increase the robustness of the system. The preview feed-forward controller, which includes the desired and disturbance signals, is used to improve the transient response of the system. A space vector pulse-width modulation (PWM) control technique for voltage source-fed IM is prepared for microprocessor-based control. Spectral analysis of the output voltage is evaluated to predict the effect of the proposed space vector modulation technique on the dynamic performance of the IM. The optimal preview controlled system is implemented, and its applicability and robustness are demonstrated by computer simulation and experimental results.**

***Index Terms*—Induction motor (IM), optimal preview control, speed control, vector control.**

I. Introduction

UNTIL more recently, induction motors (IMs) have performed the main part of many speed control systems and found usage in several industrial applications because they demonstrate trouble-free operation for long periods of time. The advances in microprocessors and power electronics have permitted the implementation of modern techniques for induction machines, such as field-oriented control [1], [5]–[7], slip frequency control [2], indirect field control [3], and vector control [1], [3]–[7]. Applications of modern control theory to IMs, such as optimal control [1], [5], adaptive control [6], variable structure control [7], neural network [8] and [9], direct torque control [9] and [10], and others, have more recently been published. There are two important points for the speed control of IMs. The first is the capability of highly accurate speed control, whereas the second is to maintain a constant speed, even if subject to disturbances. A field-oriented control technique is synthesized in this article using the vector method that requires deriving the state equation of the three-phase IM on the synchronous frame. The IM is composed of three-input and three-output variables. The input variables are the stator angular frequency and the two components of the stator space voltage vector, whereas the output variables are the rotor angular velocity and the two components of the stator space flux linkage. The objective of the controlled system is to achieve rotor speed control, field orientation control, and constant flux control. Using a new error system technique rectifies the adverse phenomena that are caused by parameter uncertainties and unmodeled dynamics. A supplementary way to improve the transient response of the controlled system is the preview feed-forward controller. This controller uses few future values of the desired and disturbance signals. The desired signal is the required rotor angular velocity and the required two components of the stator space flux linkage. The disturbance signal is the mechanical load torque subjected to the IM. A space vector PWM control technique for voltage source-fed IM is prepared for microprocessor-based control. Spectral analysis of the output voltage is evaluated to predict effect of the proposed space vector modulation (SVM) technique on the dynamic performance of the IM [11]. This technique has improved the total harmonic distortion and increased the range of obtainable fundamental voltages, without requiring large storing memories. Extensive computer simulations are made to demonstrate the robustness and feasibility of the proposed controlled system.

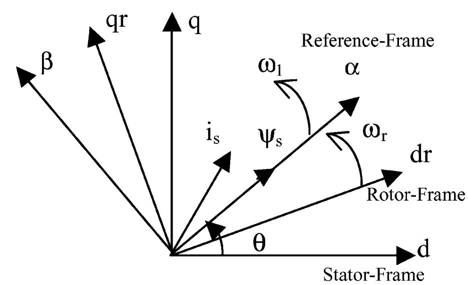

Fig. 1. Space vector representation.

II. Induction Motor Model

The state space model of the three-phase IM is derived on the basis of the vector method [5], where the reference frame is taken as the synchronously rotating frame. The dynamic equation of the IM is derived on the basis of Fig. 1, where the reference frame (α-β) is rotating at angular velocity (ω_1), with respect to the fixed-stator reference frame (d-q), whereas the rotor reference frame (dr-qr) is rotating at the rotor angular velocity (ω_r).

The state space model of the three-phase IM can be derived on the basis of the vector method in a synchronously rotating

Manuscript received June 4, 2002; revised October 22, 2004. This work was supported by the King Fahd University of Petroleum and Mines, Dharan, Saudi Arabia. Paper no. TEC-0130-2002.

M. M. M. Negm is with the Faculty of Engineering, Ain-Shams University, Abbasia, Cairo, Egypt (e-mail: mmnegm@yahoo.com).

J. M. Bakhashwain and M. H. Shwehdi are with the Department of Electrical Engineering, King Fahd University of Petroleum & Minerals, Dhahran, 31261 Kingdom of Saudi Arabia (KSA) (e-mail: jamilb@kfupm.edu.sa).

Digital Object Identifier 10.1109/TEC.2005.858072

reference frame as [1]:

$$v_s = r_1 i_s + \frac{d\psi_s}{\mathrm{dt}} + j\omega_1\psi_s \tag{1}$$

$$v_r = r_2 i_r + \frac{d\psi_r}{\mathrm{dt}} + \mathrm{j}\omega_s\psi_r \tag{2}$$

$$\psi_s = L_s i_s + L_m i_r \tag{3}$$

$$\psi_r = L_m i_s + L_r i_r \tag{4}$$

$$T = \frac{3}{2} p I_m(\psi_s^* i_s) = J\frac{d_{\omega_r}}{\mathrm{dt}} + F_{\omega_r} + T_L \tag{5}$$

where

v_s, i_s	stator space voltage and current vectors;
v_r, i_r	rotor space voltage and current vectors;
ψ_s	stator space flux vector;
ψ_r	rotor space flux vector;
T, T_L	mechanical torque and load torque, respectively;
J, F	moment of inertia and viscous friction, respectively;
$\omega_s = \omega_1 - \omega_r$	slip angular frequency of IM;
ω_1, ω_r	stator and rotor angular frequencies, respectively;
r_1, r_2	stator and rotor resistances per phase, respectively.

The linearized state space model of the three-phase IM is derived from (1)–(5), as given by [1]:

$$\frac{dx(t)}{dt} = \bar{A}x(t) + \bar{B}u(t) + \bar{C}d(t). \tag{6}$$

The output equation is selected as

$$y(t) = Ex(t) \tag{7}$$

where we have the equation at the bottom of the page. The state variable $x(t)$, the input variable $u(t)$, the output variable $y(t)$, and the disturbance signal $d(t)$ are given by

$$x(t) = [\omega_r(t)\psi_{s\alpha}(t)\psi_{s\beta}(t)i_{s\alpha}(t)i_{s\beta}(t)]^t$$
$$u(t) = [\omega_1(t)v_{s\alpha}(t)v_{s\beta}(t)]^t$$
$$y(t) = [\omega_r(t)\psi_{s\alpha}(t)\psi_{s\beta}(t)]^t;\ d(t) = T_L(t)$$
$$v_s(t) = v_{s\alpha}(t) + jv_{s\beta}(t);\ i_s(t) = i_{s\alpha}(t) + ji_{s\beta}(t)$$
$$\psi_s(t) = \psi_{s\alpha}(t) + j\psi_{s\beta}(t).$$

III. Control Law

The objective of the field orientation control is to keep the magnitude of the stator flux linkage constant while the position of rotor angular frequency changes arbitrarily. This orientation can be achieved by adjusting the stator space voltage vector and the stator frequency arbitrarily. Therefore, to achieve the previous objective, the flux component $\psi_{s\beta}$ must be equal zero, whereas the flux component $\psi_{s\alpha}$ is kept constant to attain maximum torque with changing the stator voltage components $v_{s\beta}$ and $v_{s\alpha}$ simultaneously.

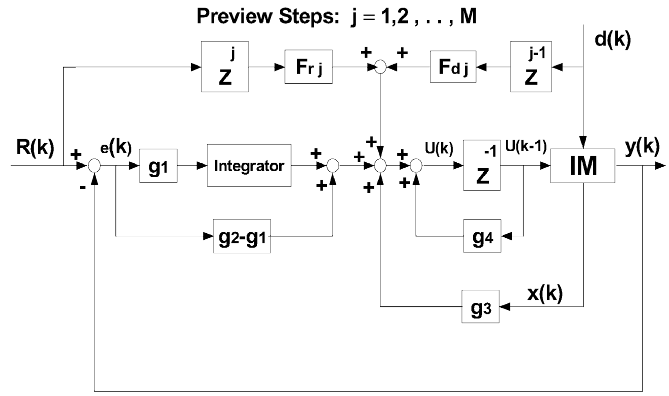

Fig. 2. Optimal preview control system.

The discrete-time equations of (6) and (7) are

$$x(k+1) = Ax(k) + Bu(k-1) + Cd(k) \tag{8}$$

$$y(k) = Ex(k) \tag{9}$$

where k represents the sampling time kT, T is the sampling period, and the dimensions of matrices A, B, C, and E are (5×5), (5×3), (5×1), and (3×5), respectively. The input vector u(k) is delayed by one sampling period to compensate for the execution time of the microprocessor.

The optimal preview control law is synthesized according to the MIMO system as follows:

$$e(k) = R(k) - y(k) \tag{10}$$

where $e(k) = [e_{\omega r}(k)e_{s\alpha}(k), e_{s\beta}(k)]^t$, and the reference signal is $R(k) = [\omega_r^d(k)\psi_{s\alpha}^d(k)\psi_{s\beta}^d(k)]^t$. The superscript "d" denotes the desired value, and "t" is the transposition.

Using (9) to get the first difference of (10) and then the substitution from (8) gives

$$\Delta e(k+1) = \Delta e(k) + F_a\Delta x(k) + F_b\Delta u(k-1) + F_c\Delta d(k) + \Delta z(k+1) \tag{11}$$

where

$$F_a = F(A - I_5); F_b = FB;\ F_c = FC;\ F = -E$$
$$\Delta z(k+1) = \Delta R(k+1) - \Delta R(k);\ \Delta = (1 - q^{-1}).$$

Then, error system (12) is constructed from (8) and (11):

$$X(k+1) = \Phi X(k) + \theta u(k) + G_r\Delta z(k+1) + G_d\Delta d(k) \tag{12}$$

$$\begin{matrix}\bar{A} = \bar{a}_{ij}, i = {}_{1,5}, j = 1,5; \bar{B} = \bar{b}ij, i = 1,5, j = 1,3; \\ \bar{C} = \bar{c}i1; i = {}_{1,5}\end{matrix};\quad E = \begin{bmatrix} 10000 \\ 01000 \\ 00100 \end{bmatrix}.$$

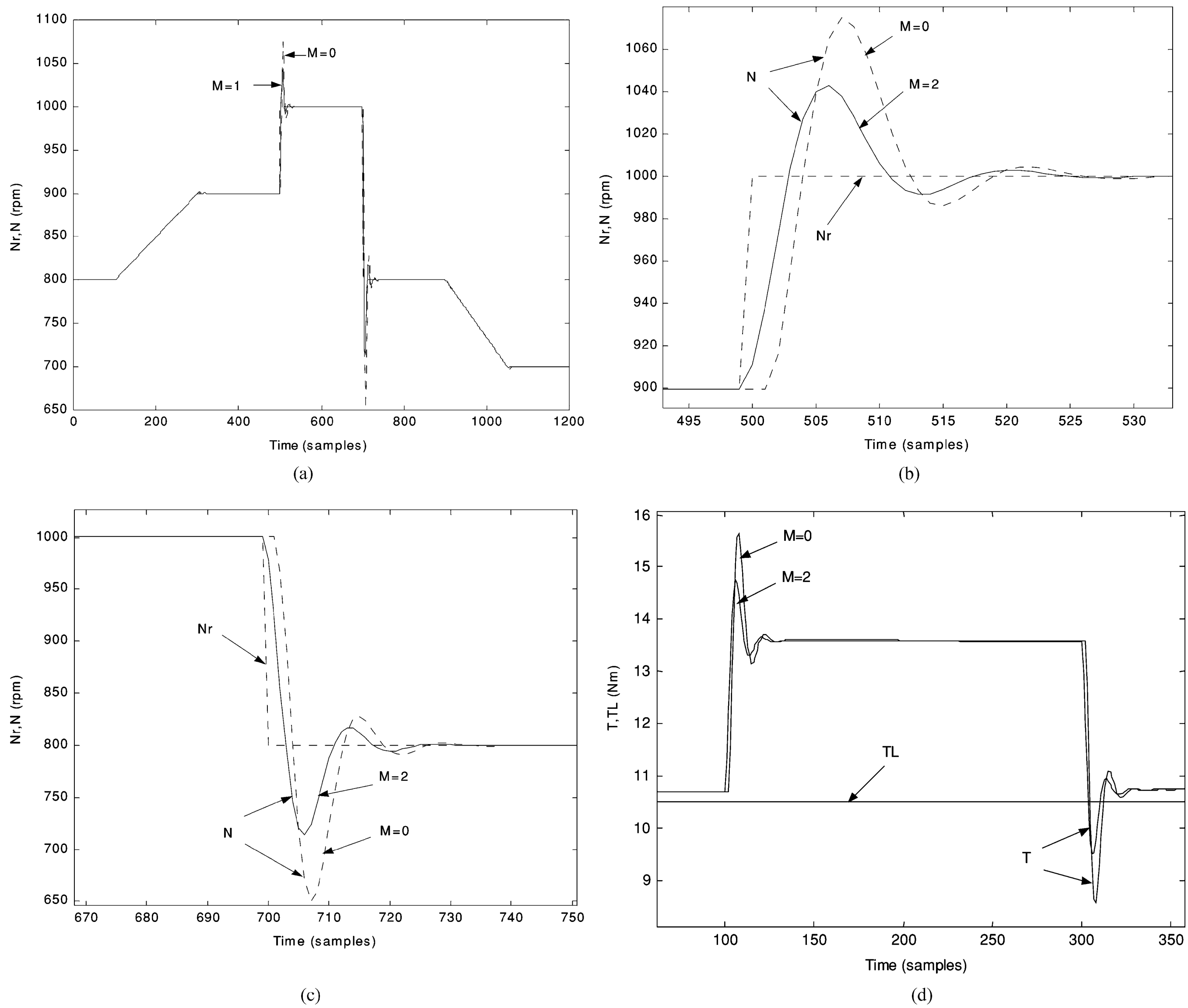

Fig. 3. Optimal preview controller response (speed variation-ramp/abrupt change).

where

$$X(k+1) = [e(k)\Delta e(k+1)\Delta x(k+1)\Delta u(k)]^t$$

$$\Phi = \begin{bmatrix} I_3 & I_3 & 0 & 0 \\ 0 & I_3 & F_a & F_b \\ 0 & 0 & A & B \\ 0 & 0 & 0 & 0 \end{bmatrix}; \ \theta = \begin{bmatrix} 0 \\ 0 \\ 0 \\ I_3 \end{bmatrix}$$

$$G_r = \begin{bmatrix} 0 \\ I_3 \\ 0 \\ 0 \end{bmatrix}; \ G_d = \begin{bmatrix} 0 \\ F_c \\ C \\ 0 \end{bmatrix}.$$

To implement the optimal preview control law, the following selected performance index J_d is to be minimized subject to the constraints given by (12):

$$J_d = \sum_{k=0}^{\infty}[X(k+1)^t Q X(k+1) + \Delta u(k)^t R \Delta u(k)]$$

where the weighting matrices Q (14×14), R (3×3), and q (3×3) are given by

$$Q = \begin{bmatrix} q & q & 0 \\ q & q & 0 \\ 0 & 0 & 0 \end{bmatrix}; \ q = \begin{bmatrix} q_1 & 0 & 0 \\ 0 & q_2 & 0 \\ 0 & 0 & q_3 \end{bmatrix}$$

$$R = \begin{bmatrix} r_1 & 0 & 0 \\ 0 & r_2 & 0 \\ 0 & 0 & r_3 \end{bmatrix}.$$

Accordingly, the minimization process gives the following optimal preview controller:

$$\Delta u(k) = GX(k) + G_1 W(k+1) + \sum_{j=2}^{M}[G_j [K_1]^{j-2} W(k+j)] \tag{13}$$

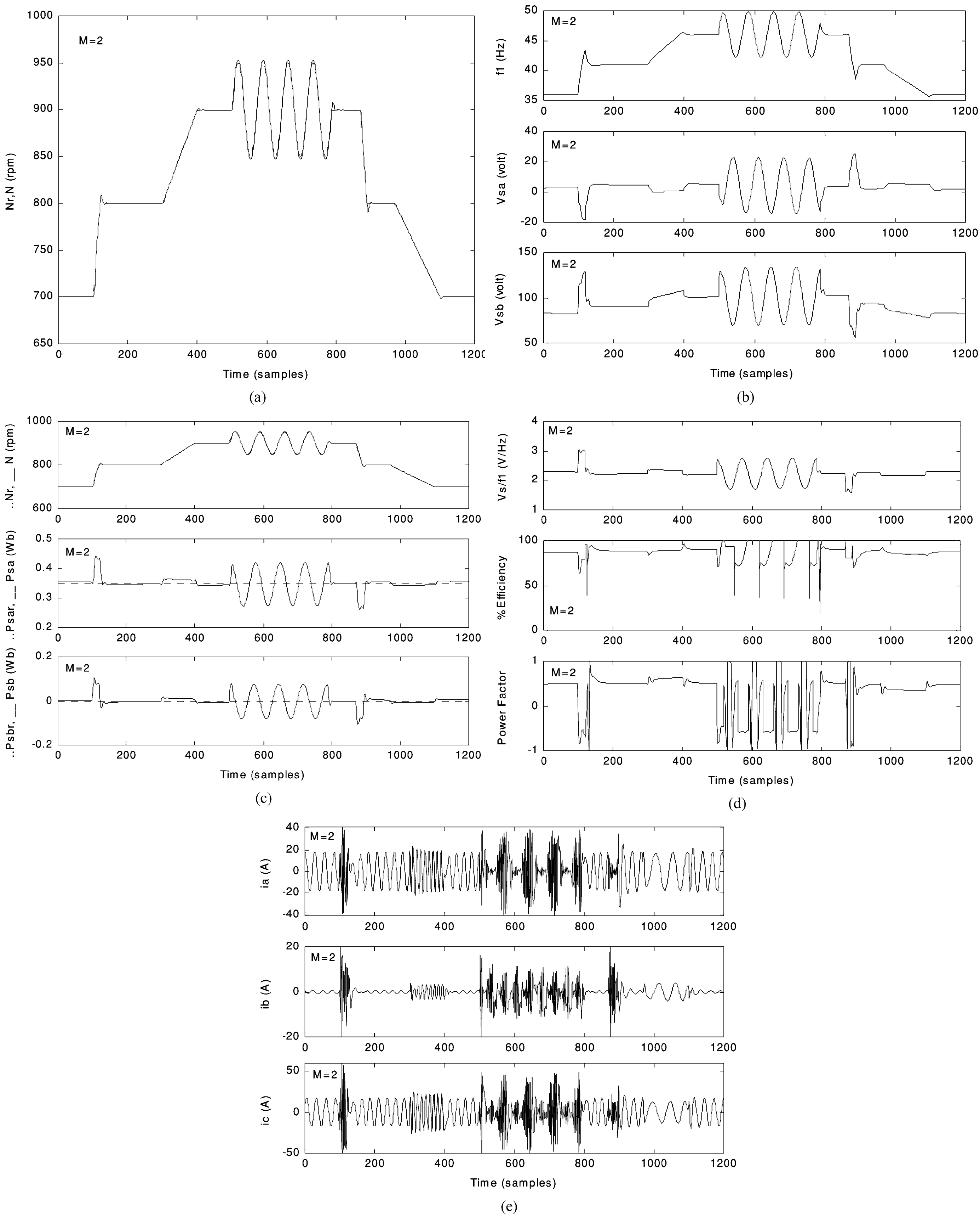

Fig. 4. Optimal preview controller response (speed variation-ramp/sinusoidal change).

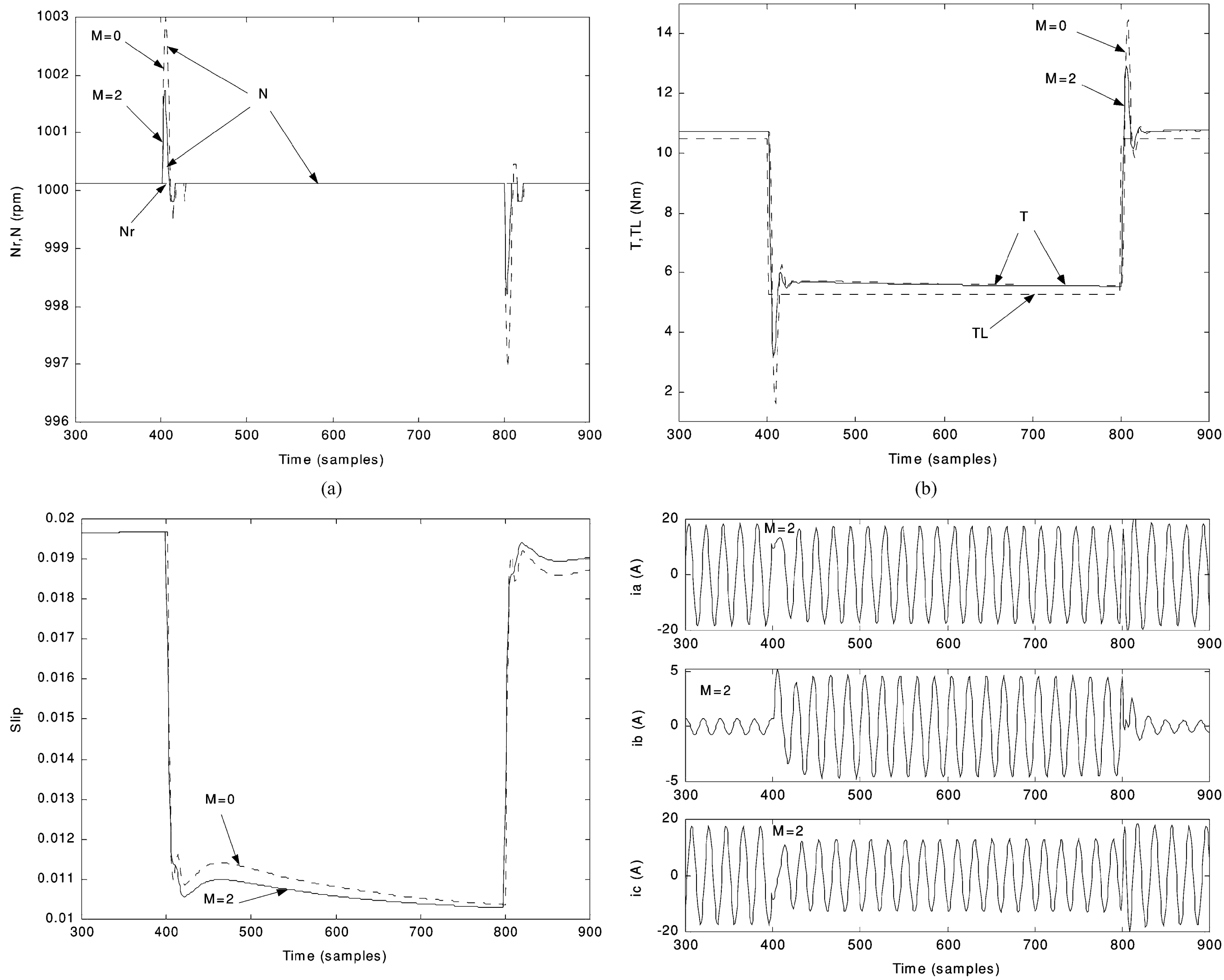

Fig. 5. Optimal preview controller response (load torque variation).

where

$$
\begin{aligned}
&W(k+1) = G_r \Delta z(k+1) + G_d \Delta d(k)\\
&\text{Feedback gain} \quad G = [g_1 g_2 g_3 g_4] = -\gamma \theta^t K \Phi\\
&\text{Feed–forward gain} \quad G_1 = -\gamma \theta^t K\\
&G_2 = -\gamma \theta^t \Phi^t \lambda\\
&G_i = G_{i-1} K_1; \quad I = 3, 4, \ldots, M.
\end{aligned}
$$

$K_1 = K^{-1}\Phi^t\lambda$, and K, γ, and λ are the steady-state solution of the following Riccati equation:

$$
\begin{aligned}
K(i) &= Q + \Phi^t \lambda(i+1)\Phi\\
\lambda(i+1) &= K(i+1)[I_{14} - \theta\gamma(i+1)\theta^t K(i+1)]\\
\gamma(i+1) &= [R + \theta^t K(i+1)\theta]^{-1}.
\end{aligned}
$$

The real-time optimal preview controller can be derived by induction from (13), such that

$$
\begin{aligned}
u(k) = {} & g_1 \sum_{i=0}^{k} e(i) + (g_2 - g_1)e(k) + g_3 x(k)\\
& + g_4 u(k-1) + \sum_{i=1}^{M} F_{ri}[\Delta R(k+i) - \Delta R(i)]\\
& + \sum_{i=1}^{M} F_{di}[d(k+i-1) - d(i-1)] \qquad (14)
\end{aligned}
$$

where

$$F_{ri} = G_i G_r;\; F_{di} = G_i G_d; i = 1, 2, \ldots, M.$$

$M \geq 1$ is the preview feed-forward steps.

The control system structure is implemented from (14), as indicated in Fig. 2.

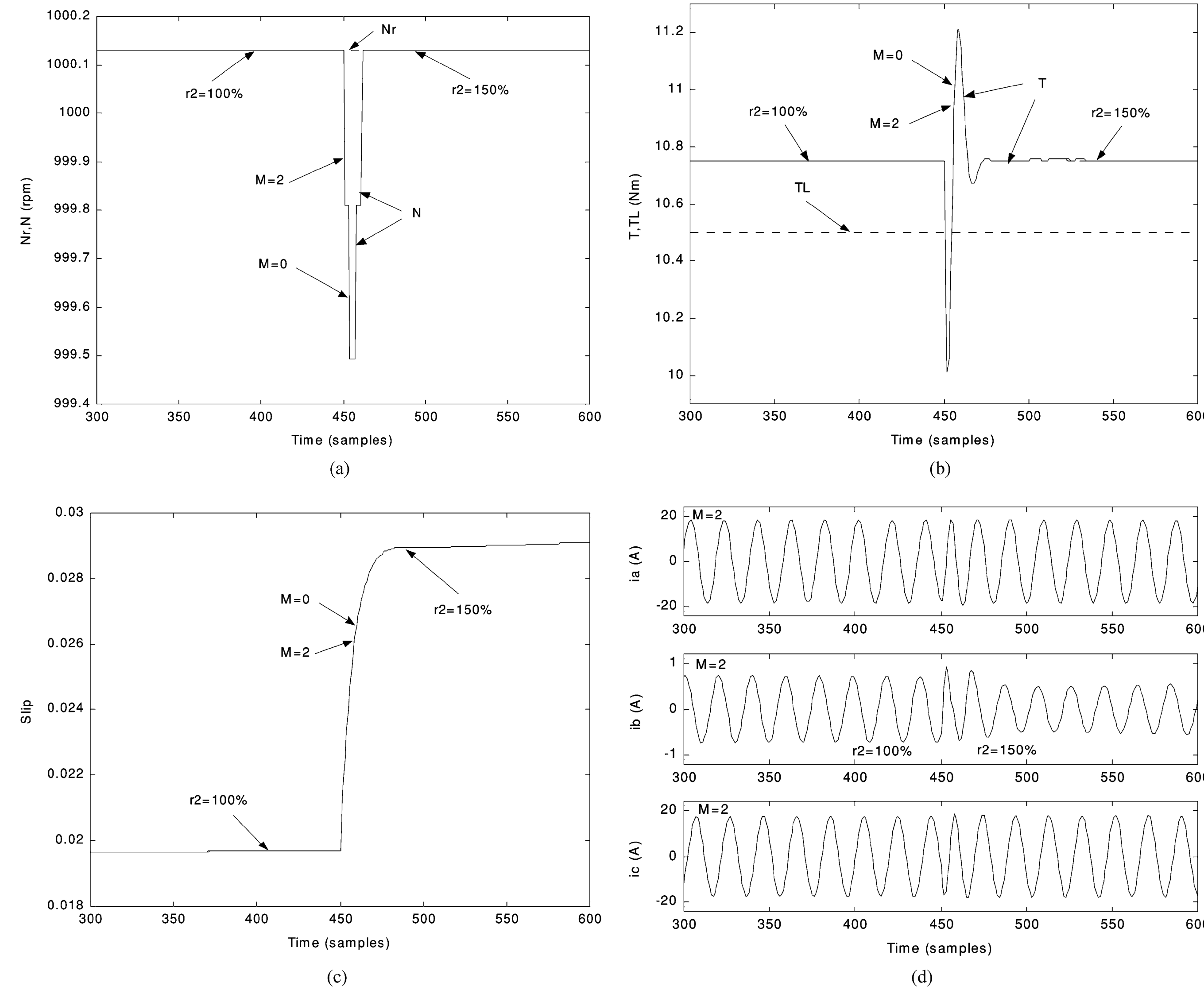

Fig. 6. Optimal preview controller response (rotor resistance variation).

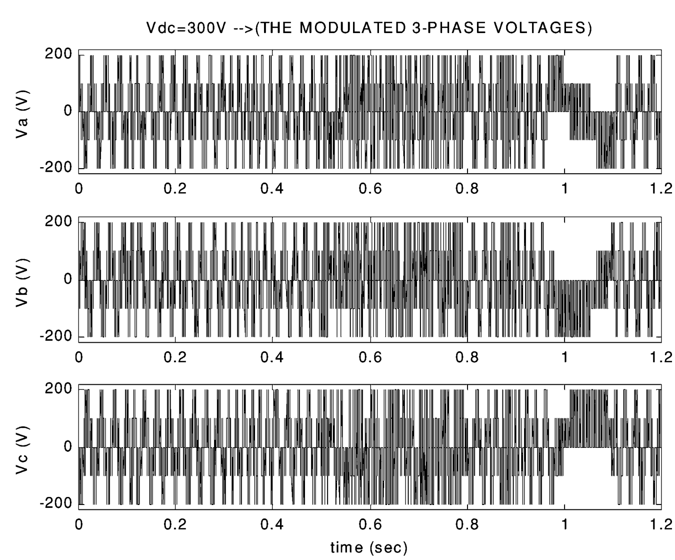

Fig. 7. Modulated stator voltages at switching $\text{frequency} = 2$ KHz.

IV. Simulation and Experimental Results

The proposed optimal preview controller is used in this paper to control a 1.1-kW, 1000-r/min, 200-V line voltage, six-pole, 50-Hz, three-phase squirrel cage IM. Its parameters are $J = 0.0179$ Kg-m^2, $F = 8E - 4$ Nm/rad/s, $r_1 = 0.2842\ \Omega, r_2 = 0.2878\ \Omega, L_m = 26.8$ mH, $L_s = 28.3$ mH, $L_r = 28.8$ mH, $\psi^d_{s\beta} = 0$, and $\psi^d_{s\alpha} = 0.35$ weber (Wb).

The MATLAB simulation results shown in Figs. 3 to 7, as well as the experimental results shown in Fig. 8, are obtained on the basis of (14) with sampling time $T = 1$ ms. The horizontal line in these figures represents the time in samples. Effect of the optimal preview controller is indicated with preview steps $M = 0$ or 2, and weight factors are $r_1 = r_2 = r_3 = 1; q_1 = 10, q_2 = q_3 = 2$.

Figs. 3(a)–(c), 4(a), 5(a), and 6(a) indicate the desired rotor speed N_r (r/min) dotted lines and its response N (r/min) in solid lines with $M = 2$, and in dashed lines when $M = 0$. Fig. 3(b) and 3(c) are enlarged parts of Fig. 3(a). The load torque T_L (Nm)

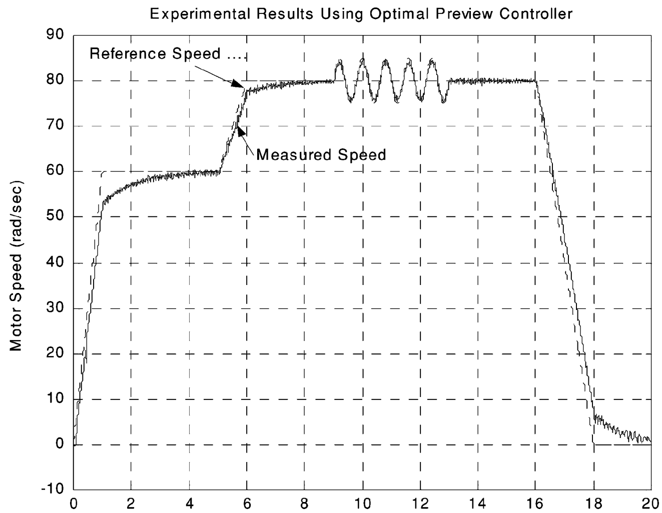

(a)

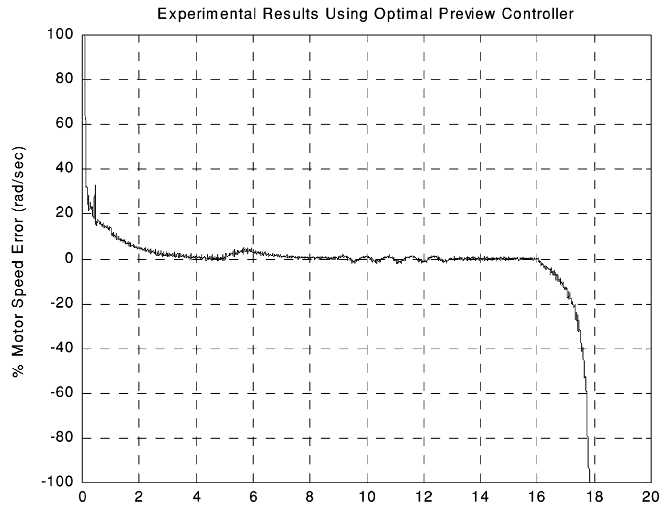

(b)

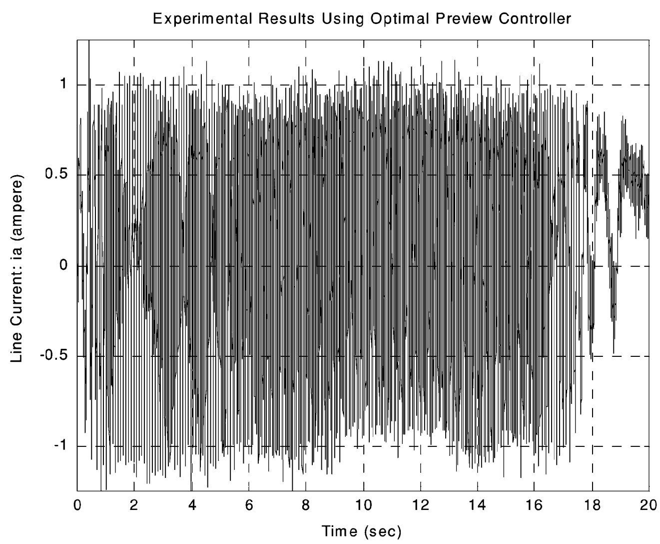

(c)

Fig. 8. Experimental results. (a) Motor speed response at light load. (b) % output error at light load. (c) Stator current at light load.

is indicated in dotted lines and the corresponding mechanical torque T (Nm) in solid lines with $M = 2$, and in dashed lines if $M = 0$, as illustrated in Figs. 3(d), 5(b), and 6(b). Figs. 3(a)–(d) are obtained at $M = 0$ and 2, with changing the desired rotor speed (N_r) gradually from 800–900 r/min and abruptly from 900–1000 r/min and back to 800 and 700 r/min, while maintaining the load torque (T_L) constant at 10.5 Nm. In Fig. 4(a)–(e) at $M = 2$, the desired rotor speed is changed gradually from 700–800 r/min and to 900 r/min with different decline, and then sinusoidally changed around 900 r/min, and gradually back to 800 and 700 r/min, while the load torque constant at 10.5 Nm. The load torque is abruptly changed from 10.5–5.25 Nm and back to 10.5 Nm, while the desired speed is kept constant at 1000 r/min, as illustrated in Fig. 5(a)–(d), at $M = 0$ or 2. Furthermore, in Fig. 6(a)–(d), at $M = 0$ or 2, the rotor resistance (r_2) is selected to change from 100% to 150% at the sampling instant 450, while maintaining the desired speed constant at 1000 r/min and the load torque constant at 10.5 Nm. The control input u(k) in (14), stator frequency f1, and the two components of the stator space voltage vector $(v_{s\alpha} = V_{sa})$ and $(v_{s\beta} = V_{sb})$ are illustrated in Fig. 4(b). The output signal y(k) and its desired value R(k) in (10), the rotor speed (N, Nr), and the two components of stator space flux vector $(\psi_{s\alpha} = \mathrm{Psa}, \psi_{s\alpha}^d = \mathrm{Psar})$ and $(\psi_{s\beta} = \mathrm{Psb}, \psi_{s\beta}^d = \mathrm{Psbr})$ are demonstrated in Fig. 4(c), where the desired values are indicated by dotted lines. Moreover, the voltage-to-frequency ratio $(Vs/f1)$, the percentage efficiency (%Efficiency), and the overall power factor are indicated in Fig. 4(d). Furthermore, the instantaneous three-phase stator currents (i_a, i_b, i_c) are demonstrated in Fig. 4(e). Figs. 4(e), 5(d), and 6(d) are drawn at $M = 2$; in addition, the motor slip (Slip) is depicted in Figs. 5(c) and 6(c) at $M = 0$ and 2. Finally, the space vector PWM technique is implemented to control the IM, using the proposed controller under the case of changing the motor speed as in Fig. 4(a), the load torque as in Fig. 5(b), and rotor resistance as in Fig. 6. The output performance of this technique is depicted in Fig. 7, which illustrates the modulated stator voltages (v_a, v_b, v_c) at switching frequency of $Fo = 2$ KHz, and a dc link inverter voltage of V $_{dc} = 300$ V [11]. As indicated from these results, a robust performance for the IM is achieved, and the transient response is improved using two preview steps $(M = 2)$ of the proposed optimal preview controller.

To indicate the feasibility of the proposed controller, the experimental results using the proposed controller with light mechanical load at 1-KHz switching frequency are shown in Fig. 8. Fig. 8(a) illustrates the speed response corresponding to the given desired speed (dotted line), whereas Fig. 8(b) depicts the percentage error of the motor speed. The corresponding stator current of phase a (i_a) is demonstrated in Fig. 8(c).

V. Conclusion

A synthesized method for speed control of a three-phase IM based on the optimal preview control theory is proposed. The vector method is adopted in the control law to simplify the controlled system analysis. The preview feed-forward steps are introduced in the control law to improve the transient response. The robustness of the controlled system is indicated by changing the rotor resistance and the load torque. A maximum torque is obtained over the whole control range by equating the β -axis component of the stator space flux to zero. Coincidental results between the desired signals and their responses are achieved. A space vector PWM control technique for voltage source-fed IM is prepared for microprocessor-based control. Spectral analysis of the output voltage of the SVM technique indicated improvements of the dynamic performance of IM. The proposed technique is found to be suitable for optimal preview control of IM. Extensive simulation results are made for speed control, field orientation control, and constant flux control. The experimental results indicate the applicability and robustness of the proposed optimal preview control system.

References

[1] M. M. M. Negm, "Torque optimized speed control of a 3-phase induction motor," in *Proc. Int. Conf. Power System Technol., PowerCon'2000*, vol. 1, 2000, pp. 67–72.

[2] R. D. Lorenz, "Tuning of field oriented induction motor controllers for high performance applications," *IEEE Trans. Ind. Appl.*, vol. 31, no. 4, pp. 812–822, Jul. 1995.

[3] F. J. Lin, R. J. Shieh, and S. S. Fu, "Decoupled stator flux oriented induction motor with fuzzy neural network uncertainty observer," *IEEE Trans. Ind. Elec.*, vol. 47, no. 2, pp. 356–367, Apr. 2000.

[4] R. C. Healey, S. Williamson, and A. C. Smith, "Improved cage rotor models for vector controlled induction motors," *IEEE Trans. Ind. Appl.*, vol. 31, no. 4, pp. 812–822, Jul. 1995.

[5] M. M. M. Negm, S. A. Leithy, H. Dora, and A. Kamel, "Vector control for a three phase induction motor based on optimal regulator theory," in *Proc. IEEE Africon'96*,, 1996, pp. 654–660.

[6] M. M. M. Negm, "Adaptive vector control for a three-phase induction motor," in *Proc. IEEE-ICIT' 96 Int. Conf. Industrial Technology*, vol. 1, 1996, pp. 762–766.

[7] T. M. Nasab and M. M. M. Negm, "Robust performance for induction motor using VSC systems with free chattering," in *Proc. IFAC-IFIP-IMACS Conf. Control of Industrial Systems*, 1997, pp. 223–229.

[8] M. M. M. Negm and A. H. Mantawy, "An ANN optimal preview controller technique for induction motor," in *Proc. IEEE Int. Conf. Industry Applications*, vol. 2, 2000, pp. 966–971.

[9] P. Z. Grabowski, M. P. Kazmierkowski, B. K. Bose, and F. Blaabjerg, "Simple direct torque neuro-fuzzy control of induction motor drives," *IEEE Trans. Ind. Electron.*, vol. 47, no. 4, pp. 83–91, Aug. 2000.

[10] J. Maes and J. A. Melkebeek, "Speed-sensorless direct torque control of induction motor using an adaptive flux observer," *IEEE Trans. Ind. Appl.*, vol. 36, no. 3, pp. 778–785, May 2000.

[11] M. M. Negm, "SVPWM verification for ANN optimal control of induction motor," in *Proc. 37th Int. Universities Power Engineering Conf. UPEC2002*, Stafford, U.K., Sep. 2002, pp. 488–493.

[12] A. Purcell and P. P. Acarnley, "Enhanced inverter switching for fast response direct torque control," *IEEE Trans. Power Electron.*, vol. 16, no. 3, pp. 382–389, May 2001.

Mohamed M. M. Negm (M'93–SM'02) was born in Cairo, Egypt, in 1956. He received the B.Sc. (Honors, First-rank), M.Sc., and Ph.D. degrees in electrical engineering from Ain-Shams University, Cairo, in 1979, 1983, and 1990, respectively.

Since 1979, he has been with the Department of Electrical Engineering, Faculty of Engineering, Ain-Shams University. From 1985 to 1989, he was granted a Japanese scholarship at the Department of Electrical Engineering, Faculty of Engineering, Hokkaido University, Sapporo, Japan. From 1992 to 2002, he was on a loan with the College of Technology, Dammam, Saudia Arabia. Since 2000, he has been with the Department of Electrical Engineering, Faculty of Engineering, Ain-Shams University, where he is currently a Professor of control of power and electrical machines. Since 2004, he has been with the Electrical and Electronics Engineering Technology Department, Yanbu Industrial College, Royal Commission for Jubail and Yanbu, Saudi Arabia. His research interests include the interdisciplinary areas of optimal preview, VSS, ANN, and adaptive control system theories and their applications, control of power systems, control of electrical machines and robotics, control of power electronic systems, advanced process control design, digital control systems, sensorless control, and applications of PLC and microprocessors in industry.

Jamil M. Bakhashwain received the Ph.D. degree from the University of Colorado, Boulder, in 1989.

He is an Associate Professor and Chairman of the Electrical Engineering Department at King Fahd University of Petroleum and Minerals, Dhahran, Saudi Arabia. His area of interests are control systems and their application and measurements and management of magnetic fields on transmission lines. He has been involved in the research and measurements of electromagnetic fields of high-voltage transmission lines. He has published many journal and conference papers and authored or co-authored a number of technical reports. He has been involved in many research projects and studies regarding power systems.

M. H. Shwehdi (S'74–M'85–SM'90) received the B.Sc. degree from the University of Tripoli, Tripoli, Libya, the M.Sc. degree from the University of Southern California, Los Angeles, and the Ph.D. degree from Mississippi State University, in 1972, 1975, and 1985, respectively, all in electrical engineering.

He was a consultant to A.B. Chance Company and Flood Engineering. He held teaching positions with the University of Missouri-Columbia, University of Florida, Gainesville, and Pennsylvania State University, University Park. At present, he is an Associate Professor with the King Fahd University of Petroleum and Minerals (KFUPM), Dharan, Saudi Arabia. His research interests include power system analysis, power quality and harmonics, and analysis of over voltages on power systems.

Dr. Shwehdi is active in IEEE activities both locally and nationally. He is listed as a distinguished lecturer with the DLP of the IEEE/PES and received the 2001 IEEE/PES outstanding chapter engineer. He received the 1999 IEEE WG for standard award. He has been the IEEE/PES Saudi Arabia chapter chairman since 1999.